

Optical properties of thin lead films in the energy range 3–15.5 eV evaporated and studied in ultrahigh vacuum

J. C. Lemonnier, M. Priol, and S. Robin

Laboratoire de Spectroscopie, Université de Rennes-Beaulieu, 35031 Rennes-Cedex, France

(Received 9 April 1973)

Reflectance measurements, *in situ*, on freshly deposited thin lead films are carried out in the far uv. Optical constants and other useful functions such as ϵ_1 , ϵ_2 , $-\text{Im}(\epsilon^{-1})$, $-\text{Im}(\epsilon + 1)^{-1}$ are deduced. The existence of volume and surface plasmons is demonstrated. The structure of ϵ_2 is attributed to interband transitions both at critical points and between parallel bands; for the latter there is reasonable agreement between the experimental data and Ashcroft's calculation.

INTRODUCTION

Lead behaves like a free-electron metal because the $6s^2 6p^2$ outer-shell electrons are loosely bound to the rest of the atom. Moreover, lead being a heavy metal, a strong spin-orbit interaction is expected as shown by Louck's energy-band structure for Pb. This band scheme shows the existence of parallel bands¹ which have so far not been taken into consideration for the interpretation of the optical properties of lead.

We have reported in a previous paper² the optical properties of Pb films evaporated and studied at a pressure of 10^{-6} torr in the energy range 4–40 eV. It was interesting to carry out this study in ultrahigh vacuum, thus avoiding surface contamination and oxide formation. The latest results of this type are those of Norris and Walden³ who studied photoemission, Liljenvall *et al.*⁴ who studied the optical properties in ultrahigh vacuum in the energy range 0.6–6 eV, and Ashton and Green⁵ who measured the optical constants in the range 10–30 eV.

EXPERIMENTAL METHOD

The apparatus used for the reflectance measurements is described elsewhere⁶; 99.999%-pure lead is used in the form of a wire, 0.5 mm in diameter. It is evaporated onto Pyrex substrates by means of an electron gun, the substrates being at room temperature. The rate of evaporation is of the order of 100–200 Å/sec and the film thicknesses (≈ 1500 Å) are measured by means of an interference microscope. During the evaporation, the pressure rose to 5×10^{-8} torr and then fell to its base value ($\approx 5 \times 10^{-10}$ torr) after 2 or 3 min. The normal-incidence reflectance measurements were carried out immediately after the film formation in a vacuum of about 5×10^{-10} torr.

RESULTS

Curve 1 in Fig. 1 shows the reflectance results between 3 and 15.5 eV: It is the result of about twenty good evaporations and the time spent in data

collection with any one specimen was between 2 and 3 h. Reflectance was monitored at periodic intervals in order to check a possible effect of surface contamination of the layers. No change was observed in reflectance data during an interval of 3 h. At a total pressure of 5×10^{-10} torr, this relatively long time without contamination effect could be explained by a sticking coefficient less than unity and an absence of active gases. The residual-gas composition was determined by a quadrupole mass spectrometer. The precision of the reflectance measurements was evaluated to $\pm 1\%$. Curve 2 represents results previously obtained at a pressure

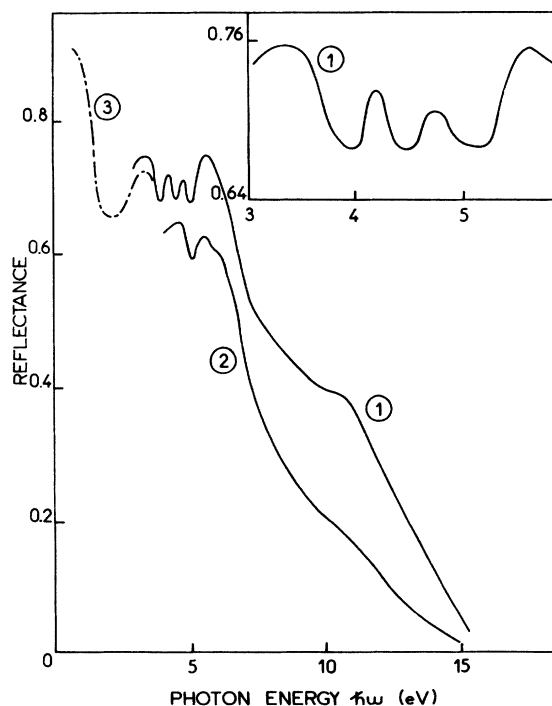


FIG. 1. Normal incidence reflectance of Pb. Curve 1: our results (ultrahigh vacuum); curve 2: our results (10^{-6} torr); curve 3: Liljenvall's results (Ref. 4).

of 10^{-6} torr. It is seen at once that the ultrahigh-vacuum results are fairly high and the structures are better defined and more numerous than in previous work; this is due principally to the absence of film contamination.⁴ Curve 3 is deduced from the optical constants measured by Liljenvall *et al.* in ultrahigh vacuum. We find quite good agreement with our results in the common region near 3 eV. The recent measurements of Ashton are slightly lower than ours in the common region 10–15 eV. It should be noted that the drop in reflectance in the present case is more abrupt than at a pressure of 10^{-6} torr and is shifted towards higher energies. The resulting calculated volume-plasma frequency will be in better agreement with value determined from the free-electron theory.

Optical constants n and k represented in Fig. 2 were obtained by Kramers-Kronig analysis of the reflectance data. The extrapolation in the lower-energy region is made with the help of the results in Ref. 4, while in the higher-energy region our previous results were used. Since it is difficult to determine the accuracy of the Kramers-Kronig analysis, we carried out reflectance measurements at various angles of incidence for about ten wavelengths and calculated optical constants by Tousey's method.⁷ The agreement is good between the two methods (within 4%).

INTERPRETATION

Figure 3 shows the curves ϵ_1 , ϵ_2 and Fig. 4 the curves $-\text{Im}(\epsilon^{-1})$ and $-\text{Im}(1+\epsilon)^{-1}$. A very sharp maximum at 13.5 eV on $-\text{Im}(\epsilon^{-1})$ curve corre-

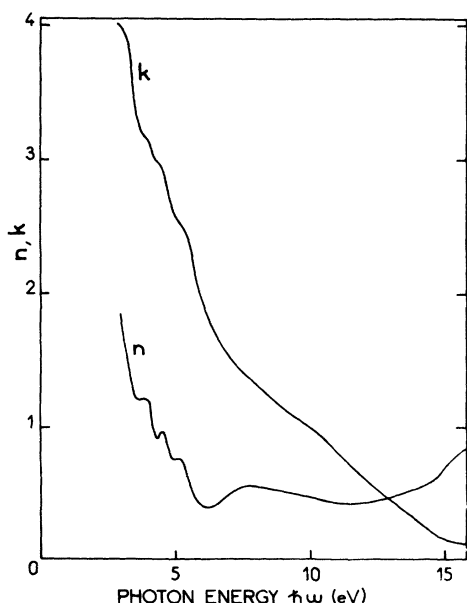


FIG. 2. Optical constants of Pb.

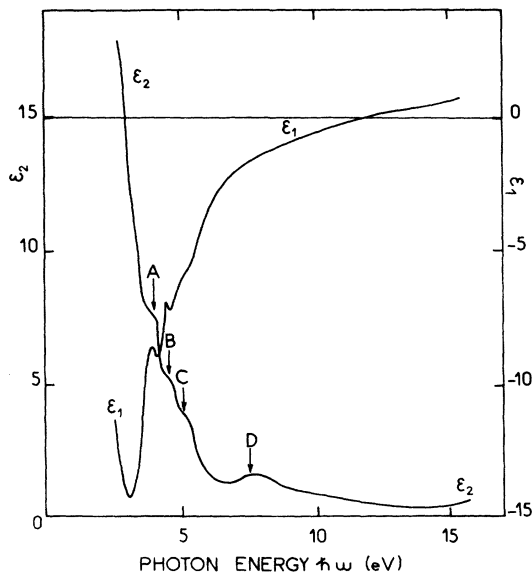


FIG. 3. Dielectric constants of Pb.

sponds to a region where ϵ_1 vanishes and ϵ_2 is small. This is characteristic of the existence of a volume plasmon. Moreover, the position of this plasmon is in good agreement with the theoretically calculated value of 13.4 eV corresponding to four valence electrons. The value of the plasmon energy obtained from measurements performed in a vacuum of 10^{-6} torr is lower (12.7 eV) than our result. Recently, a value of 12.7 eV has been reported for the plasmon energy by Ashton and Green. Finally, the agreement is quite good with measured characteristic electron energy losses.⁸⁻¹⁰ The width of the peak corresponds to a relaxation

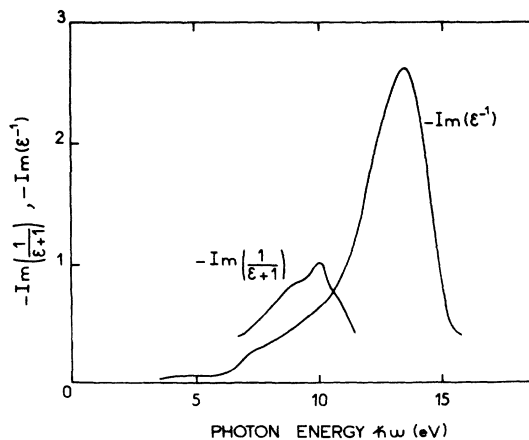


FIG. 4. Volume loss function $-\text{Im}(\epsilon^{-1})$ and surface loss function $-\text{Im}(1+\epsilon)^{-1}$.

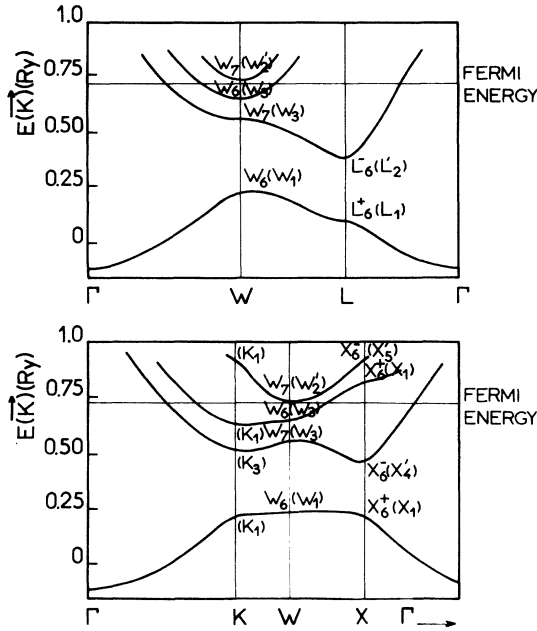


FIG. 5. Band structure of Pb from Loucks (Ref. 1).

time $\tau = 2 \cdot 10^{-16}$ sec. The curve $-\text{Im}(\epsilon + 1)^{-1}$ shows a maximum at 10 eV. Considering that ϵ_1 takes a value -1 between 9 and 10 eV and the reflectance curve shows a small drop near 10 eV, we think that there is an excitation of a surface plasmon which is due to the existence of weak roughness. Its position is in good agreement with the theoretical frequency of $13.4/\sqrt{2} = 9.5$ eV and Ref. 10.

We try to interpret the different features of the ϵ_2 curve (Fig. 3) with the help of the energy-band scheme proposed by Loucks (Fig. 5). This band scheme shows the existence of parallel bands and a distinct separation of the two lowest p bands due to strong spin-orbit interaction. It is in good agreement with the results of Anderson and Gold¹¹ and Stedman *et al.*¹² for energies close to Fermi level but at higher energies the agreement is not very good. Liljenvall *et al.*⁴ attributed the structures between 0.6 and 6 eV to the transitions from the second and the third bands to the symmetry points K , W , and X . These structures are found

to be more distinct on our curve in the region 3–6 eV. The structure (A) at 3.9 eV may be attributed to the transition $|K_1 - (K_1)|$, that at 4.5 eV (B) to the transition $|X_6^-(X_4^-) - X_6^+(X_1^+)|$, and that at 5.2 eV (C) to the transition $|K_3 - (K_1)|$ which confirms Rasigni's hypothesis.¹³ The transitions at higher energies (D) do not appear to be perfectly established from the work on photoemission, but it should be noted that the position of the lowest bands differs considerably according to different authors.^{1,12} A transition from the bottom of the third band seems to be possible to a K point, the minimum being situated at 1.1, 1.0, and 1.2 eV below the Fermi level according to Loucks, Anderson, and Gold, and Norris and Walden, respectively. We can therefore make the hypothesis that the maximum at 7.7 eV can be attributed to a transition between a level (K_1) to a level K situated in an empty band at about 6.6 eV above the Fermi level. It is also possible that a transition $W_6(W_1)$ to $W_7(W_2')$ takes place at 7.7 eV. In this case, our data are in better agreement with the Louck's band scheme. Nevertheless, it is difficult to know the exact position of the conduction band from the band scheme.^{1,12}

Moreover, according to the results of Harrison,¹⁴ Golovashkin,¹⁵ and Ashcroft and Sturm,¹⁶ the existence of parallel bands in polyvalent metals can give rise to appreciable absorption in addition to the transitions associated with the stationary values of the interband state density $\nabla E_{i,j}(k) = 0$. The parallel bands are separated by an energy $2U(K, T)$, where $U(K, T)$ is the Fourier component of pseudopotential at temperature T . Figure 6 shows different theoretical and experimental curves representing the variation of conductivity $\sigma = nk\nu$ as a function of photon energy. Curve 1 corresponds to the experimental curve of Liljenvall *et al.* and curve 2 gives our results. Curve 3 represents the variation of the theoretical conductivity calculated from Drude's theory (relaxation time $\tau = 0.60 \cdot 10^{-15}$ sec), which is calculated using experimental values of the dielectric function in the infrared. In order to calculate the ratio m/m_{opt} , which is involved in the relation giving the Drude contribution to the optical conductivity, we have used the following relation¹⁶:

$$1 - \frac{m}{m_{opt}} = \sum_K \frac{1}{2} \frac{K}{2k_F} \frac{|U_K|}{E_F} \left\{ \left[\frac{1}{2} \pi - \sin^{-1} \left(\frac{2U_K}{\hbar\omega_0} \right) \right] + \frac{|U_K|}{2E_K} \left[\frac{\omega_0}{2\omega_1} + \frac{3\omega_1}{2\omega_0} - 2 - \ln \left(\frac{\omega_1}{\omega_0} \right) \right] \right\},$$

where

$$\hbar\omega_0 = 2(E_K E_F + U_K^2)^{1/2} - E_K$$

and

$$\hbar\omega_1 = 2(E_K E_F + U_K^2)^{1/2} + E_K$$

which gives $m/m_{opt} = 0.617$.

The curves 4 were calculated according to Eq. (10) in Ref. 16 making use of the numerical data of Anderson and Gold.¹¹ These curves represent the contribution to σ of transitions between parallel bands. For lead, the maxima on these curves are

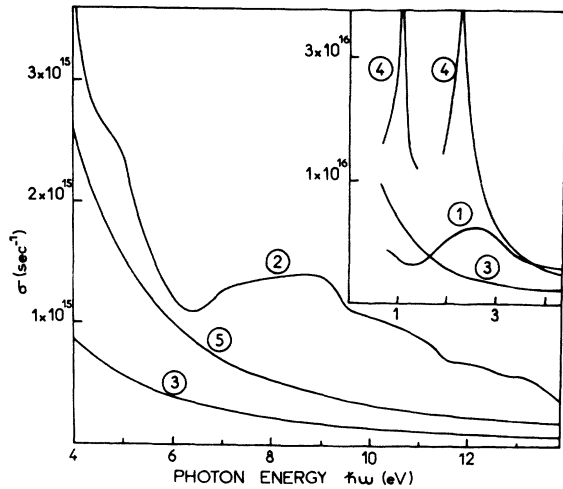


FIG. 6. Comparison of the observed interband conductivity with that predicted in the Drude's theory. Curve 1: Liljenvall's results; curve 2: our results; curve 3: Drude's theory; curve 4: Ashcroft's theory without collisions; curve 5: parallel bands contribution.

expected to be at energies corresponding to $2|U_{200}|$ and $2|U_{111}|$, that is, at 1.1 and 2.3 eV, respec-

tively. A weak structure is observed at about 1 eV and a large maximum towards 2.5 eV on the experimental curve. It is thus likely that these structures are due to transitions between parallel bands. Curve 5 shows the contribution to the calculated optical conductivity due to collision effects according to Eq. (19) in Ref. 16. This equation involves the relaxation time τ_i corresponding to the transitions between the parallel bands. We tried different values of τ_i in Eq. (19) in order to approach closely the experimental results of Liljenvall *et al.*,⁴ which led us to choose $\tau_i = 10^{-15}$ sec. The calculated conductivity is then in good agreement with their experimental values. The difference between the two curves is less than 4% between 3 and 3.5 eV, the latter being the high-energy limit of their measurements.

Consequently, we can say that the different curves on Fig. 6 show distinctly the contributions to the conductivity of transitions between parallel bands, normal interband transitions, and the Drude term. The transitions between parallel bands introduce, in particular, two structures at low energies and a background contribution at higher energies.

¹Y. L. Loucks, *Phys. Rev. Lett.* **14**, 1072 (1965).

²P. Girault, A. Seignac, M. Priol, and S. Robin, *C.R. Acad. Sci. (Paris)* **266**, 688 (1968).

³C. Norris and L. Wallden, *J. Phys. F* **2**, 180 (1972).

⁴H. G. Liljenvall, A. G. Mathewson, and H. P. Myers, *Philos. Mag.* **22**, 243 (1970).

⁵A. M. Ashton and G. W. Green, *J. Phys. F* **3**, 179 (1973).

⁶J. C. Lemonnier, J. Thomas, and S. Robin, *J. Phys. E* **6**, 553 (1973).

⁷R. Tousey, *J. Opt. Soc. Am.* **29**, 235 (1939).

⁸W. Klein, *Optik (Stuttg.)* **11**, 226 (1954).

⁹L. B. Leder, *Phys. Rev.* **103**, 1721 (1956).

¹⁰C. J. Powell, *Proc. Phys. Soc. Lond.* **76**, 593 (1960).

¹¹J. R. Anderson and A. V. Gold, *Phys. Rev.* **139**, 1459 (1965).

¹²R. Stedman, L. Almquist, G. Nilsson, and G. Raunio, *Phys. Rev.* **163**, 567 (1967).

¹³G. Rasigni, J. P. Codaccioni, J. Michaud-Bonnet, F. Abba, and J. P. Petrakian, *C.R. Acad. Sci. B* **262**, 772 (1966); F. Abba, J. P. Codaccioni, J. Michaud-Bonnet, J. P. Petrakian, and G. Rasigni, *C.R. Acad. Sci. B* **262**, 954 (1966).

¹⁴W. A. Harrison, *Phys. Rev.* **147**, 467 (1966).

¹⁵A. I. Golovashkin, A. I. Kopeliovich, and G. P. Motulevich, *Zh. Eksp. Teor. Fiz.* **53**, 2053 (1967) [*Sov. Phys.-JETP* **26**, 1161 (1968)].

¹⁶N. W. Ashcroft and K. Sturm, *Phys. Rev. B* **3**, 1898 (1971).